Available online at www.sciencedirect.com
ScienceDirect
BioSystems xxx (2006) xxx–xxx
Bio Systems
www.elsevier.com/locate/biosystems

Getting into shape: Optimal ligand gradients for axonal guidance

Jean-Philippe Thivierge [a,*], Evan Balaban [b]

[a] *Département de physiologie, Université de Montréal, Canada*
[b] *Department of Psychology and Behavioral Neurosciences Program, McGill University, Canada*

Received 28 July 2005; received in revised form 2 July 2006; accepted 2 July 2006

Abstract

During neural development, neurons from downstream, presynaptic regions of the nervous system (such as the retina) send spatially patterned axonal projections to upstream, target regions (the tectum or superior colliculus). A *servomechanism model* has been proposed to explain the pattern and time-course of axonal growth between these two regions [Honda, H., 1998. Topographic mapping in the retinotectal projection by means of complementary ligand and receptor gradients: a computer simulation study. J. Theor. Biol., 192, 235–246]. Here, we show that a modification of this model incorporating a different criterion for axonal decision-making, called the *local optimum rule*, is guaranteed to converge to a topographic map under a wide range of conditions encountered during neural development. A theoretical investigation of these conditions leads to new hypotheses regarding map formation.

Keywords: Axonal guidance; Ephrin; Retinotopic map; Servomechanism model

1. Introduction

When interviewed by a reporter from the Boston Globe shortly after winning the Nobel Prize in 1981, the neurophysiologist David Hubel stated, "There has been a myth that the brain cannot understand itself, the brain or the mind. It is compared to a man trying to lift himself by his own bootstraps. We feel that is nonsense. The brain can be studied just as the kidney can" (McLaughlin, 1981). One implication of this statement is that it should be possible to articulate lawful rules encapsulating particular aspects of brain structure and function that can lead to a deeper understanding of how the brain works. In this view, neural science requires its practitioners to integrate theoretical and empirical evidence to advance the understanding of a particular topic. In our case, this topic concerns how orderly patterns of connections between cells in brain circuits are formed. Starting from a small set of embryonic neural precursor cells, human brains end up with a complex organized network estimated to contain about 100 billion (10^{11}) neurons with 10 quadrillion (10^{16}) synapses. These synaptic connections are not formed at random. According to what principles do neurons establish patterned connections?

Many regions of the brain receive organized sets of connections from other brain regions. Some of the best-described examples are regions that receive visual information. The neural part of the eye, the retina, creates a mosaic of information about the pattern of light stimulation that falls upon it. Neurons from the retina connect to other areas of the brain, predominantly the midbrain (called the tectum or superior colliculus; SC) and the thalamus. These projections have fascinated scientists for years, because the spatial relations between neighboring neurons in the retina set up a map of the visual world, and that map is retained by the orderly set of projections between presynaptic cells in the retina, and

* Corresponding author. Tel.: +1 514 3436111x3202; fax: +1 514 3436113.
E-mail address: jean-philippe.thivierge@umontreal.ca (J.-P. Thivierge).

0303-2647/$ – see front matter © 2006 Elsevier Ireland Ltd. All rights reserved.
doi:10.1016/j.biosystems.2006.07.001

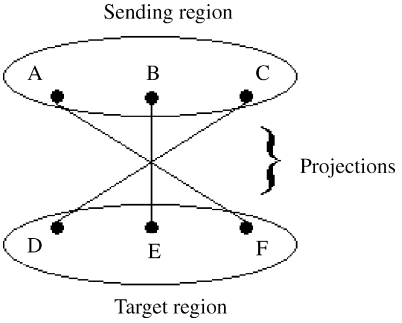

Fig. 1. Projections from a sending to a target region.

postsynaptic cells in the SC and thalamus. For decades, scientists have tried to uncover the mechanisms by which retinal axons are guided to their correct locations within a target region.

1.1. Retinotopic organization

Through the course of development, a large number of axons travel from the presynaptic sending region (the retina) to a postsynaptic target site (e.g., the SC). This mass of axons will be referred to as the *projections* from a sending to a target site. These projections have several interesting characteristics (Fig. 1). First, the relative spatial relationship between sites of the sending and target regions is maintained. This means that, if two points are close together on the sending region, they will remain close together on the target region. Conversely, this also means that if two points are distant from one another on the sending region, they will remain distant on the target region. This characteristic is known as *topography*. Another characteristic of projections is *polarity*. This attribute describes possible transformations that the projections perform on the distribution of points at the sending site. In Fig. 1, the projections produce a mirror image of the sending region onto the target region, thus resulting in a *reversed* polarity. The topography and polarity of projections can be described independently of one another; it is possible to have different kinds of topographic relations combined with different kinds of polarities. In the retinal projections of the visual system, for instance, topographically faithful representations are combined with a reversed polarity. In contrast, somatosensory projections conveying touch information to the brain are topographic, but polarity is not reversed.

1.2. Molecular gradients

One goal of growing axons is to locate regions where they will form synaptic connections with other neurons in the brain. At the tip of the developing axon is a motile structure termed the *growth cone* that senses the concentration of chemical signals (Gordon-Weeks, 2000). If the chemical signal exists in a concentration gradient, signal concentrations may act as road signs, dictating the direction in which the axon should travel next, and where it should ultimately stop and connect with other neurons. Axons can have different types of receptors at their tips, causing them to respond to different types of signals. Among axons responding to the same signals, axons can differ in the concentrations of receptors on their tips, which determine their sensitivity to chemical concentration cues, in turn leading the axons to stop at different places on the gradient.

While the above account relies on molecules that are expressed as gradients, it was not clear until recently what these molecules were, and whether they existed as gradients of freely diffusing molecules or as gradients of molecules that are attached to cell surfaces. Roger Sperry's *chemoaffinity hypothesis* (Sperry, 1963) proposed that topographic map formation could be specified by molecular labels expressed in a position-dependent manner across the projecting and target areas. However, this hypothesis was silent with respect to the functional characteristics of such labels. It was not until the mid-1990s, with the identification of Eph/ephrin molecules, that the mechanisms by which such a system could potentially operate began to be understood (Palmer and Klein, 2003). Eph/ephrins are complementary receptor and ligand molecules normally bound to the cell surface that are part of the receptor tyrosine kinase family. Although these cell-to-cell signaling molecules had been identified previously in other contexts, it was only relatively recently that evidence started linking them to axonal guidance. Several characteristics of the Eph/ephrin complex make then well suited for guiding axons. First, these signaling molecules are expressed in concentration *gradients* in target regions of the nervous system. Second, the growth cones of traveling axons are differentially sensitive to concentrations of Eph/ephrins because their level of receptor expression depends on the spatial location they come from, leading to concentration-dependent effects on the movement of the axons in accordance with their spatial position of origin.

One of the most interesting features of traveling axons is the possibility that topographically faithful projections may be obtained without a need for electrical activity in the projecting cells. It is not clear if spontaneous activity is present from the earliest stages of mammalian development, and exactly what its role in map formation is (cf., Ruthazer and Cline, 2004). The position argued for here is that there exists an initial stage of retinotopic

Please cite this article in press as: Thivierge, J.-P., Balaban, E., Getting into shape: Optimal ligand gradients for axonal guidance, BioSystems (2006), doi:10.1016/j.biosystems.2006.07.001

development where the largest influence on map formation is given by activity-independent cues (Thivierge and Balaban, 2005). In this view, Eph/ephrin molecules can guide axons to their initial topographic positions. Then, at a later stage, the dynamic maintenance of these connections becomes at least partially dependent upon neural activity, endowing these projections with an ability to respond plastically to any changes an organism may undergo (for a discussion of classic experiments on the flexibility of this system, see Fraser and Perkel, 1990).

Recent empirical findings on the role of guidance molecules have led to increasingly detailed theoretical and mechanistic accounts of axonal guidance (Yates et al., 2004; Reber et al., 2005; for a review see Goodhill and Xu, 2005). However, one of the best models of this process remains the servomechanism model of Honda (1998, 2003). Using a simple yet elegant and biologically grounded principle, this model is able to account for the detailed time-course of axonal growth under normal conditions, as well as reproducing the results of several experiments using "knock-out" mice, where the influence of Eph/ephrin molecules is removed or attenuated. Overall, the servomechanism model is recognized as one of the most detailed attempts yet to address recent EphA and ephrin-A misexpression data. However, some of its assumptions lack empirical grounding, and have thus been deemed arbitrary by some researchers (Goodhill and Xu, 2005). One of the goals of the current work is to motivate some of these assumptions mathematically, particularly with respect to gradient shapes and retinotectal interactions. First, the servomechanism model will be described in detail. Second, we will address different ways of generating a stop signal, as well as different shapes of ligand gradients on the target surface, and different ways in which they may influence growing axons. Third, the convergence of axons to optimal termination zones (TZs) will be demonstrated. Finally, ways to generate interstitial branching will be explored.

2. Servomechanical guidance

The servomechanism model provides a good theoretical account of the relative precision of the initial, activity-independent projections (Honda, 1998, 2003; see also Loschinger et al., 2000). In particular, the servomechanism model offers an account of how an axon gradually extends its growth cone through a target surface in the midbrain (the model does not describe migration of the growth cone along the optic tract to get to the midbrain). The direction in which the growth cone will move is determined mainly by chemotropic factors, but also by stochastic exploration and competitive cell–cell interactions (based on competition for growth- or survival-related "neurotrophic" factors secreted by postsynaptic cells). Chemotropic factors influence migration through their interaction with the growth cone receptors. Through its interactions with the target surface, the growth cone will aim towards a position where all its receptors are occupied. This position is referred to as the point of maximum receptor saturation. The servomechanism model proposes that cells compute the difference between the actual position of the axon on the target surface, and the location of its best possible TZ.

When determining their final TZ on the target surface, growth cones make use of two pieces of information. The first piece of information depends jointly upon the receptor concentration expressed at the tip of the growth cone, and the concentration of ligand molecules at the present location. The receptor concentration is dependent upon the gradient of expression of receptor molecules $R(u)$ where $u = \{1,2,\ldots,N\}$ is a position along one dimension of the sending region. The concentration of ligand molecules is dependent upon the gradient $L(v_t)$ on the target surface, where $v_t = \{1, 2, \ldots, N\}$ describes a dimension of the target region, and t is a time-step of migration. This notation assumes that, while the position of the axon on the target surface can change as a function of time, its position on the sending surface remains constant. According to the *law of mass action*, describing the kinetics of receptor–ligand interactions, the result of this interaction is a *topographic signal* G obtained by a second-order kinetic equation:

$$G(u, v_t) = R(u)L(v_t). \quad (1)$$

Here, we take $R(u)$ and $L(v_t)$ to reflect a summation over multiple receptor and ligand interactions. As opposed to other formulations (e.g., Goodhill, 1998a,b), this means that there is no requirement to sum this equation over multiple receptor and ligand interactions, because the receptor and ligand functions employed are already taken to be a summation over all molecular interactions.

The second piece of information, the *saturation limit* of the growth cone, is used to determine the final TZ. Recall that the growth cone senses out concentrations of molecules in its environment. However, the growth cone is only sensitive to concentration changes below a certain limit (defined by a variable M_u). When put together, the topographic signal $G(u, v_t)$ and saturation limit M_u can be used to determine the best TZ according to the following equation (for each migration step):

$$d(u, v_t) = |G(u, v_t) - M_u|, \quad (2)$$

or, less concisely, $d(u, v) = |R(u)L(v_t) - M_u|$. In this equation, $d(u, v_t)$ provides a measure of the distance

Please cite this article in press as: Thivierge, J.-P., Balaban, E., Getting into shape: Optimal ligand gradients for axonal guidance, BioSystems (2006), doi:10.1016/j.biosystems.2006.07.001

between the current location as indicated by the topographic signal, and maximum receptor saturation. According to the servomechanism model, the larger this distance, the farther away an axon is from its best (herein referred to as "optimal") position on the target surface. This measure is computed independently for each traveling axon, and each dimension of migration along the two-dimensional target surface.

In the proposed approach, the maximum receptor saturation M_u is made directly dependent upon receptor density $R(u)$, by setting $M_u = (R(u))^2$. Because M_u is meant to reflect second-order interactions between receptor and ligand densities, it is plausible that it be set in this fashion. As a consequence, the direction of migration of the axon will be directly dependent upon the receptor density of the growth cone. With this definition, Eq. (2) becomes

$$d(u, v_t) = L(v_t) - R(u). \tag{3}$$

If $d(u, v_t)$ increases following a given migration step, the axon retracts to v_t (i.e., the position of the axon prior to migrating on this given step). For each given axon, migration continues until a stop signal is reached.

In the absence of a stop signal (see following section), the axon migrates to a new position in the target surface according to $v_{t+1} = v_t \pm 1$. Here, the $\pm$ sign determines the direction of migration (forward versus backward). For each given migration step, this sign is determined randomly.

In the servomechanism model, an axon progresses across a target surface by taking "steps". At each of these steps, a decision is made to either keep going, or retract. To make this decision, the axon first computes d_{start} (the distance at the start location before the step is taken) according to Eq. (3). Then, the axon moves to the new position, and calculates d_{end} (the distance at the finish location) according to the same equation. If the new position has a lower d value ($d_{\text{start}} > d_{\text{end}}$), the axon will possibly remain there, according to a Gaussian probability of

$$p(d_{\text{start}}) = \exp\left[\frac{-d_{\text{start}}^2/(2\sigma^2)}{\sqrt{2\pi\sigma}}\right].$$

Otherwise, if the new position has a higher d value than the start position, the axon will retract to the start position and initiate a new migration step. While in the original servomechanism model (Honda, 1998) the probability of moving is given by

$$\frac{p(d_{\text{end}})}{p(d_{\text{start}}) + p(d_{\text{end}})},$$

in the current work we assume that $p(d_{\text{end}}) = 1$ for simplicity.

The mechanism whereby an axon retracts if d increases possesses a key advantage: it guarantees that, through its motion across the target surface, the axon will never increase its distance d. However does this guarantee that the axon will always try to *decrease* its distance d? This question will be addressed by describing how an axon determines a stopping position in the target surface.

3. Generating a stop signal

How does the cell determine the best possible TZ for a given axon? Even though Eq. (3) provides us with an idea of how far an axon is from its best possible location on the target surface, it does not specify how the axon knows when to stop. Two main proposals for a stop signal have emerged. According to the first proposal (the *set-point rule*), the axon stops when the topographical signal G reaches a pre-determined constant c, i.e., $G \approx c$. While biologically reasonable, this is an ad hoc assumption. An alternative, called the *local optimum rule* (Thivierge and Balaban, 2005), proposes that a stop signal is generated when the ligand gradient "flattens out". Let's look at an example. In Fig. 2, we graph a plausible ligand gradient (Goodhill, 1998a,b):

$$L(v_t) = \frac{\alpha}{-1 + \exp(\beta v_t) + \alpha},$$

where α and β are free parameters. The concentration of ligand molecules produced by this gradient reduces steadily up to a certain point (i.e., around $v_t = 10$), and then remains almost constant near zero. At this point, there is no reason for an axon to choose one location beyond 10 over another, because $L(v_t)$ remains almost constant, so d will not change much. Thus, it is preferable to just stop around the point where the gradient becomes flat. Formally, according to the local optimum

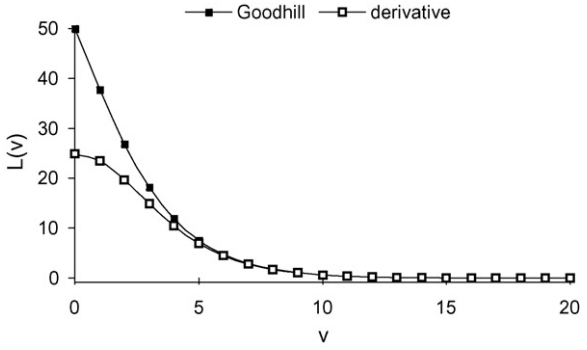

Fig. 2. Goodhill (1998a,b) gradient and derivative. $\alpha = 100$; $\beta = -0.5$.

Please cite this article in press as: Thivierge, J.-P., Balaban, E., Getting into shape: Optimal ligand gradients for axonal guidance, BioSystems (2006), doi:10.1016/j.biosystems.2006.07.001

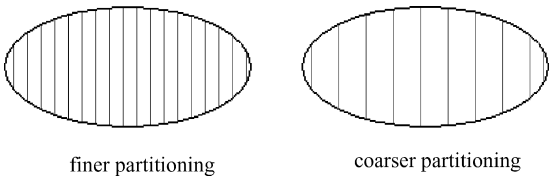

Fig. 3. A finer and coarser partitioning of the target surface is obtained by adjusting the step-size of migration.

rule, a stop signal is generated when $\partial G(u, v_t)/\partial v_t = R(u)\partial L(v_t)/\partial v_t \approx 0$.[1]

There are a several possible objections to the use of local optimum rules in generating a stop signal (Goodhill, 1998a,b; Goodhill and Urbach, 1999; Goodhill and Richards, 1999). Here, these objections will be re-evaluated according to a novel approach to generating a stop signal. As we will show, local optimum rules survive this re-evaluation. Furthermore, we are able to show that the servomechanism model, in conjunction with these rules, guarantees the convergence of traveling axons to optimal target sites.

4. Axonal migration and optimal gradients

To begin discussing whether, in the servomechanism guidance model using local optimum rules, a traveling axon is actually guaranteed to decrease its distance d, we must first analyze more closely how an axon actually travels. In the standard servomechanism model, migration occurs in steps of size $|s| = 1$, randomly determined to be either forward ($s = 1$) or backward ($s = -1$). By definition, this is the smallest possible step-size that an axon can take across a target surface. This means that the velocity of a traveling axon is always "1". There is an alternative way of conceptualizing the step-size of migration, as illustrated in Fig. 3. When the step-size is small, the traveling axon samples the target surface very finely. Conversely, if the step-size is increased, the same axon will sample the target surface in a coarser, more spread-out manner. Thus, the step-size can be viewed as a measure of how the axon partitions the target surface. This has an important implication, namely that the step-size controls sensitivity to local changes in the gradient. If the partitioning is very fine, the axon will be sensitive to every small "bump" in the gradient. However, by taking larger steps, the axon will skip a lot of the local changes in gradient density, and this may facilitate getting to a target site quicker. The proposed view of partitioning assumes the finest partitioning possible to be equivalent to the minimum detectable difference in concentration prior to reaching the maximum receptor saturation. In addition, this view acknowledges that the tectum (or SC) is a continuous surface; however, it also concedes that only a discrete sampling of tectal gradients is possible by the growth cone.

Intuitively, one can imagine that migrating in steady steps of "1" will eventually result in a final TZ, but this may take a while. What would stop a cell from making the step-size arbitrarily large? If it makes the step-size too big, the axon will overshoot its target location, and will have to retract over some distance. The larger the step-size, the more retraction will be necessary. As it turns out, researchers have found that mammalian axons have a tendency to slightly overshoot their target site, and eventually retract towards it (Yates et al., 2001, 2004). With its set-point rule, the original servomechanism model tells us nothing about what the step-size should be.

The local optimum rule can be employed to generate an adaptive step-size, determined according to $s \propto R(u)\partial L(v_t)/\partial v_t$ (Thivierge and Balaban, 2005). The step-size will be larger when the axon is in a steep portion of the gradient, and smaller when it is in a shallow portion. If the axon is experiencing a steep portion of its gradient, it is likely to be nowhere near its optimal site (a formal demonstration of this will be presented in Section 5). Therefore, the axon can travel quickly and confidently through this region. However, if the axon is experiencing a ligand gradient that is rather flat, the axon is near an optimal site and should take smaller and smaller steps to minimize overshooting.

To see how the local optimum rule can be employed to determine the step-size s, we start with a simple case where $s = \text{sign}(R(u)\partial L(v_t)/\partial v_t)$, resulting in $s = -1$ or 1. Although this simple strategy does not stretch the step-size beyond "1", it makes the direction of migration non-random. We can further refine this simple case by making the derivative control the size of steps so that they do not always take on a value of "1". This can be achieved by setting $s = k(R(u)\partial L(v_t)/\partial v_t)$ – the step-size becomes directly proportional to the derivative of the ligand function, scaled by a constant k. This simply displaces the step-size problem onto a variable k – how should such a variable be set? There are two ways to answer this question, namely with respect to the optimal solution, and with respect to how an axon can plausibly assess such a parameter. First, we will address the former question; we will see that the answer to the second question is closely related.

[1] This equation shows that it is not so much that a stop signal is generated when the ligand gradient flattens out, but rather when the topographic signal stops fluctuating; however, these two observations are directly related.

Please cite this article in press as: Thivierge, J.-P., Balaban, E., Getting into shape: Optimal ligand gradients for axonal guidance, BioSystems (2006), doi:10.1016/j.biosystems.2006.07.001

Is there a way to set k such that the axon takes the smallest number of steps? We can determine the number of steps necessary for a given migration through the following function:

$$f(s) = \frac{|R(u)L(v_t) - M_u|}{s} + 2s. \quad (4)$$

Here, the number of steps is proportional to the initial distance between the topographic signal and the maximum receptor saturation. The factor of $2s$ is added to describe the initial overshoot and retraction of the axon around an optimal location.

The next step involves an assumption that R and L are linear. This step is taken for simplicity; in fact, as we will demonstrate below, the optimal L is not linear. With the assumption of linearity, we reduce Eq. (4) to

$$f(s) = \frac{|uv_t - M_u|}{s} + 2s. \quad (5)$$

Based on this equation, the smallest number of steps for a given migration can be obtained by differentiating with respect to s, and then solving for s. First, differentiating with respect to s results in the following:

$$f'(s) = |uv_t - M_u|(-s^{-2}) + 2, \quad (6)$$

where $f'(s) = \partial f(s)/\partial s$. Second, solving for s, we obtain:

$$s = \sqrt{0.5|uv_t - M_u|}. \quad (7)$$

This equation provides us with the optimal step-size to take, such that the migration will occur in the least possible number of steps.

Now that the optimal step-size is known precisely, we turn to the question of evaluating whether it can be approximated using the local optimum rule. If we retain our assumption of linearity for the receptor and ligand gradients, the stop signal can be reduced in the following way: $R(u)\partial L(v_t)/\partial v_t = u$. Given this result, we can compare the optimal step-size solution (on the left) to the local optimum rule (on the right):

$$\sqrt{0.5|uv_t - M_u|} \propto u. \quad (8)$$

It is easy to see that this proportionality holds. Thus, the local optimum rule results in a step-size that is proportional to the optimal solution of Eq. (7). However, there are some important distinctions between the two methods; most notably, the optimal solution takes into account the maximum receptor saturation of the growth cone. The distinction between the optimal step-size and local optimum rule can be isolated by a simple mathematical transformation, by making $k = s/u$, or, expanded:

$$k = \frac{\sqrt{0.5|uv_t - M_u|}}{u}, \quad (9)$$

yielding $ku \propto u$. Defined in this way, the factor k reveals a direct way to get from an approximated local optimum step-size to an optimal step-size.

But how could an axon compute this value of k? Remember that, in all the above calculations, we worked under the assumption that the function representing the ligand gradient was linear. This assumption is arbitrary: it makes more sense to ask the developing axons what would be the best function for them to use to obtain the value of k. Thus, we seek a ligand function such that $ku = L(v_t)u$; this function turns out to be simply:

$$L(v_t) = \frac{\sqrt{0.5|uv_t - M_u|}}{u}. \quad (10)$$

Fig. 4a illustrates various possible ligand gradients based on this function; they resemble the gentle followed by precipitous decay characteristic of many biological diffusion patterns. Although Eq. (10) is a monotonically decreasing function along the anterior (A)–posterior (P) dimension (i.e., A > P; representative of EphA3–A7), it could also be possible to generate increasing functions by taking $1/L(v_t)$, thus representing other forms of gradients (i.e., A < P; representative of ephrin-A2, -A5, and -A6) (McLaughlin and O'Leary, 2005). The advantage of using Eq. (10) as a general form of ligand density function is that it guarantees attainment of the target site in the smallest number of steps. This signal may emerge through the interaction of several molecular gradients (see Section 7 for ways to combine multiple gradients).

In sum, Eq. (10) offers a mathematical justification for a particular shape of molecular signal; others may be possible, yet they will not attain the target site in the smallest number of steps within the current framework (whether or not this condition is strictly imposed in biological systems remains to be explored). These other possibilities will not be considered further. In the next section, we consider some of the key implications of Eq. (10). Then, in Section 5, we explore how an optimal TZ can be reached using Eq. (10).

4.1. Effective gradients

One of the properties of the ligand density function described in Eq. (10) is that it is dependent on the retinal position u of a projecting axon. It is plausible to assume that axons with various receptor densities project from topographically organized locations in the retina. In other words, the number of available receptors on the retinal ganglion cell (RGC) growth cones varies according to position on the retina (Hansen et al., 2004). In this way, nasal RGCs will exhibit a relatively larger number of receptors than temporal RGCs. In turn, the

Please cite this article in press as: Thivierge, J.-P., Balaban, E., Getting into shape: Optimal ligand gradients for axonal guidance, BioSystems (2006), doi:10.1016/j.biosystems.2006.07.001

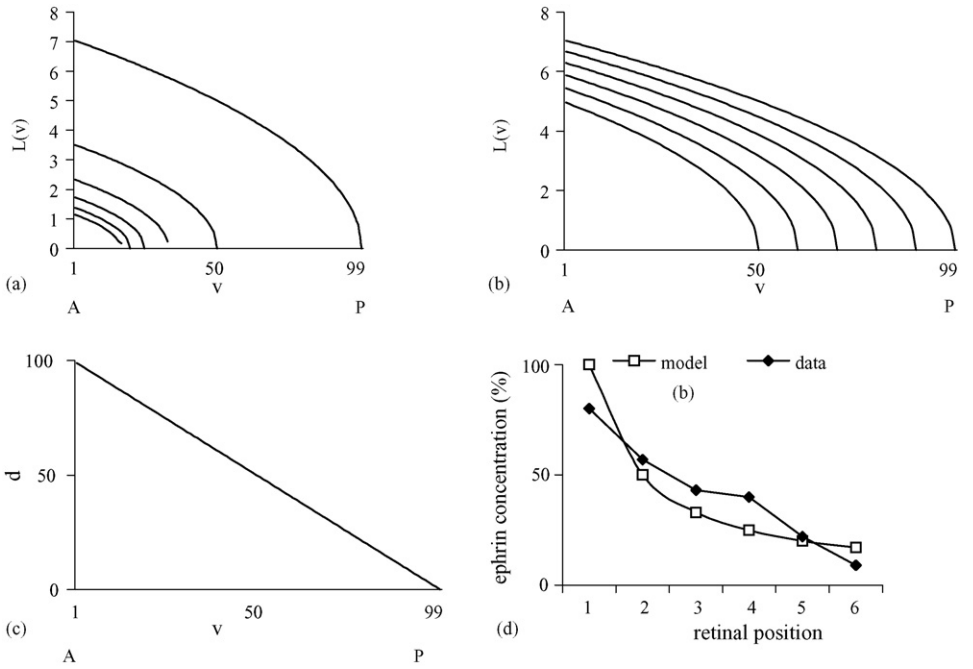

Fig. 4. (a) Ligand gradient function of Eq. (10) for different values of u (from left to right: 6, 5, 4, 3, 2, 1). For regions of the target surface, P = posterior SC; A = anterior SC. This graph shows a decreasing effective gradient where the concentration is A > P. (b) Changes in gradient with respect to M_u, with $u = 1$ (from left to right: 50, 60, 70, 80, 90, 100). (c) Corresponding decrease in distance d for $u = 1$ (similar curves are obtained for other values of u). (d) Relation between receptor position and corresponding ligand density concentration that has no net effect on axon outgrowth.

varying number of receptors of RGC growth will determine the influence of guidance molecules on the target surface. Different concentrations of SC gradients will be detected depending on the number of receptors present on a growth cone (Hansen et al., 2004). For instance, if a migrating growth cone quickly fills all its available receptors, it will no longer be able to detect increases in molecular concentrations on the target surface.

The proposed idea that different gradients can be obtained depending on the initial local conditions of the sending surface is compatible with recent empirical evidence. One recent study explored the influence of ephrin-A2 on the motion of axons on a membrane carpet (Hansen et al., 2004). In a series of in vitro assays, retinal cells taken from different regions of the eye invaded a target region of tectal cell membranes with a controlled density of ligand present. Separate assays were carried out for different ligand concentrations. One important finding from this study is that the extent to which projections grew at each ligand density depended upon the place in the retina the projecting cells were taken from. While low concentrations of retinally expressed ephrin-A2 promoted outgrowth and thus acted attractively, higher concentrations acted repulsively, and thus inhibited outgrowth. Furthermore, results demonstrated that the shift between outgrowth and repulsion depends on the origins of the fiber along the nasal–temporal axis of the retina, and is likely due to the EphA retinal gradient. In this way, nasal axons require a higher concentration of ligands in the SC to be repelled, while axons from the temporal pole are repelled by lower concentrations. This explanation is consistent with the expression of EphA3–A5 receptors along the nasal–temporal axis of the retina (Cheng et al., 1995; Feldheim et al., 1998). These results thus argue for retinal fibers seeking a region of the SC where both ephrin and Eph forces are balanced.

Thus, it may be that the shape of a gradient as sensed by the growth cone is directly dependent upon inherent features of the growth cone. As a consequence, different axons starting from various locations of the retina would experience SC gradients in a very different way. The term *effective gradient* describes these ideas. Effective gradients can be conceptualized as abstract signals taken as the sum of interactions between a growth cone and a target environment. As such, they cannot be measured directly, but rather only through their influence on the migration of the growth cone. Understanding effective gradients is perhaps the most important aspect of studying axonal guidance; however, it is still largely ignored in computational models.

Fig. 4a plots different ligand functions obtained for different values of u, while keeping M_u constant. While

Please cite this article in press as: Thivierge, J.-P., Balaban, E., Getting into shape: Optimal ligand gradients for axonal guidance, BioSystems (2006), doi:10.1016/j.biosystems.2006.07.001

the overall shape of the function remains similar, lower values of u extend the gradient out further along the anterior–posterior dimension. In addition to generating different effective gradients for different receptor densities of the growth cone, Eq. (10) makes a further prediction, namely that the effective gradient is also dependent upon the maximum receptor saturation M_u. The results of different values of M_u on the effective gradient are depicted in Fig. 4b.

The decrease in distance d through migration is depicted in Fig. 4c. This decrease is perfectly linear with increases in ligand position v_t. This means that the choice of ligand gradient proposed by Eq. (10) makes it possible to constantly decrease distance through migration. There is no stagnation of d at any point in the progression of the growth cone.

The predictions of our model are compared with empirical results in Fig. 4d. In our model, ephrin concentration is expressed as a percentage by setting 100% to be the ligand position where $L(v_t)$ reaches zero for $u = \{1, 2, 3, 4, 5, 6\}$. Overall, this model approximates the empirically observed distribution, although there are still some unresolved differences, particularly at low u values (i.e., low ephrin concentrations).

4.2. Computing a stop signal

The local optimum rule used to generate a stop signal states that an axon stops migrating when the derivative of the topographic signal $G(u, v_t)$ with respect to position on the SC surface approaches zero: $\partial G(u, v_t)/\partial v_t \approx 0$. The derivative of the topographical signal (Eq. (10)) with respect to v_t is

$$\frac{\partial L(v_t)}{\partial v_t} = \frac{0.5}{2\sqrt{|uv_t - M_u|0.5}}. \quad (11)$$

In the proposed framework, triggering a stop signal through the local optimum rule is equivalent to doing so with a set-point rule where $c = u$. When a traveling axon reaches location c in the SC, Eq. (11) falls to zero, thus triggering a stop signal. Thus, this approach proposes that a set-point rule that is dependent upon retinal position is mathematically equivalent to a local optimum rule: under certain plausible conditions, the set-point and local optimum rules can be seen as equivalent.

This framework can address a limit of the local optimum rule raised in previous theoretical work (Goodhill, 1998a). One problem with the local optimum rule is that the minimum $R(u)\partial L(v_t)/\partial v_t = 0$ may not exist at all if $\partial L(v_t)/\partial v_t$ never goes to zero. Furthermore, if it exists, then $\partial L(v_t)/\partial v_t$ goes to zero at some point, and thus $R(u)\partial L(v_t)/\partial v_t = 0$ for all retinal positions. The solution offered by Eqs. (10) and (11) is to make $L(v_t)$ directly dependent upon $R(u)$. In this case, different ligand gradients can be obtained for different receptor densities. As a result, different minima to $\partial L(v_t)/\partial v_t$ can be obtained for different axons with varying receptor densities.

5. Convergence to an optimal site

Having discussed the main properties of Eq. (10), we now address whether it is possible to prove that a traveling axon will reach an optimal site on the target region. In order to obtain any guarantee that a traveling axon will attain an optimal site on a target surface, some preliminary conditions must be stated. These conditions have to do with the state of the environment where the axon is situated. Intuitively, one can imagine that in a totally chaotic environment (one that lacks any kind of order), it would be impossible for the mailman to deliver a letter to your door. In the same way, if the environment where the axon travels was completely devoid of order, the axon would be incapable of using any cues to guide itself to its final destination. Thus, we introduce some basic environmental requirements for an axon to attain optimal target sites. We restrict ourselves to three biologically plausible requirements that are computationally sufficient to ensure guidance to optimal target sites.

Definition 1. The maximum receptor density saturation M_u is constrained to be $M_u > R(u)L(v_t)$ for every value of $u = \{1,2, \ldots, N\}$ and $v_t = \{1, 2, \ldots, N\}$.

Definition 1 states that no matter what the receptor or ligand density is, the resulting topographic signal can never, by definition, be higher than the maximum receptor saturation.

Definition 2. A given projection system involving regions u and v_t, as well as gradients $R(u)$ and $L(v_t)$, is said to be *solvable* if there exists an $L(v_t)$ such that $L(v_t) = M_u/R(u)$.

Definition 2 implies that there must exist a location on the target surface where $d = 0$. If this definition does not hold, the performance will be

$$\min_v = L(v_t) - \frac{M_u}{R(u)},$$

for a monotonically descending ligand gradient (e.g., Fig. 4a). This means that the axon would otherwise "fall off" the edge of the target surface without having found $d = 0$.

Please cite this article in press as: Thivierge, J.-P., Balaban, E., Getting into shape: Optimal ligand gradients for axonal guidance, BioSystems (2006), doi:10.1016/j.biosystems.2006.07.001

If we set $M_u = (R(u))^2$, Definitions 1 and 2 imply that there exists a region of the target area such that $R(u) = L(v_t)$. These definitions hold if both $R(u)$ and $L(v_t)$ are bounded to finite values, and if a minimum distance d exists somewhere along in the target surface.[2] It had previously been proposed that mass action models depend on the condition that $R(u) = 1/L(v_t)$ (Goodhill, 1998a). However, as seen here, it is possible that the receptor and ligand densities be proportional to one another given particular values of M_u.

Definition 3. A ligand gradient $L(v_t)$ is said to be *representative* if, at every point where $d > 0$, $\partial L(v_t)/\partial v_t \neq 0$.

If Definition 3 is respected, then by random motion, the axon will eventually explore a region of the target region where $d = 0$, providing such a region exists (see Definition 2). However, if Definition 3 is not respected, a stop signal will be generated at a location where $d > 0$. Definition 3 depends in part on the step-size of migration across the target surface. As stated earlier, a larger step-size can make the system function accurately in the face of small local imperfections on the gradient.

According to these definitions, we can deduce the convergence time of an axon. With a set-point rule, given a step-size of "1", the best possible time will be $M_u/R(u)$. However, for this to be true, every decision the axon takes must be the correct one. If, pessimistically, the axon never takes a single good decision, the convergence time will stretch to infinity, because the axon will never reach its target site.

Using a local optimum rule, we can improve both on the best and worst times of a set-point rule. First, because the step-size in no longer $s = 1$, the best time of the system can be improved, as shown in Eq. (5). Second, because steps are no longer random (i.e., they now depend on the ligand gradient), the worst time is no longer infinity. To be more precise, if Definitions 1–3 hold, the best and worst time are now both equal to Eq. (5) (or, in the more general case, Eq. (4)). We propose that, if Definitions 1–3 hold, we are guaranteed convergence to an optimal target site. This is described in the theorem below, holding Definitions 1–3 as necessary and sufficient to obtain faithful maps.

Theorem 1. *If Definitions 1–3 hold, a traveling axon using servomechanism guidance with local optimum rules is guaranteed to converge to* $d = 0$.

[2] In the case where $R(u)$ and $L(v_t)$ are not in the same range, it could be possible to restate this equation as $R(u) = \eta L(v_t)$, where η is a scaling factor.

Proof. It can be demonstrated that the axon will progress towards $d = 0$ while $\partial L(v_t)/\partial v_t > 0$, i.e., with an ascending gradient (a similar principle holds for descending gradients). Here, for simplicity, we assume linear gradients on the sending and target surfaces. However, a similar proof can be provided with non-linear gradients. If the axon is located at a point (u, v_t), distance is calculated as

$$d_{\text{start}} = |uv_t - M_u|.$$

By moving the axon according to a step of size s, the new distance can be re-calculated as

$$d_{\text{end}} = |u(v_t + s) - M_u|.$$

If a correct migration has been made, $d_{\text{start}} > d_{\text{end}}$ or, put differently:

$$|uv_t - M_u| > |u(v_t + s) - M_u|. \tag{12}$$

This equation reflects this idea that, by increasing the target site position v_t by a step of size s, we decrease distance to the optimal site. Eq. (12) will hold true if two conditions are fulfilled. First, $M_u > uv_t$, which holds true by Definition 1. Second, adding s to this equation should not change this condition, so $M_u > u(v_t + s)$. This also holds true according to Definition 1.

Thus, Eq. (12) shows that, under reasonable conditions, any given step s will decrease d. If the projection system is solvable (Definition 2), then there exists an $L(v_t)$ such that $L(v_t) = M_u/R(u)$. If the ligand gradient is representative (Definition 3), then the axon will always travel in the right direction, such that, eventually, distance will converge to

$$d = |uv_t - M_u| = |u(M_u/u) - M_u| = 0.$$

□

Note that, if the system in not solvable, the best performance will be

$$d = |uv_t - M_u| = |u \ \max(v_t) - M_u|.$$

6. Special cases

There are four special cases of ligand density functions that must be considered individually. Although these do not apply with a model that employs Eq. (10) as molecular signal, they are worth discussing to evaluate how the model would generalize to different forms of gradients.

Please cite this article in press as: Thivierge, J.-P., Balaban, E., Getting into shape: Optimal ligand gradients for axonal guidance, BioSystems (2006), doi:10.1016/j.biosystems.2006.07.001

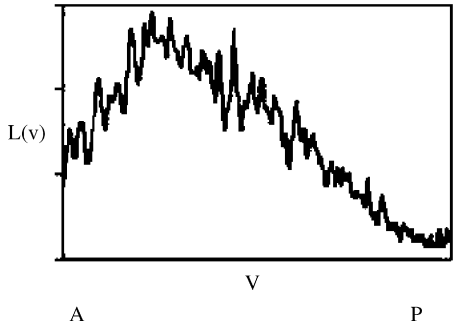

Fig. 5. Ephrin-A2 gradient from Hansen et al. (2004), using densitometric scans through the SC. The non-monotonicity of ephrin-A2 suggests two solutions for axons (at either end of the target region). P = posterior SC; A = anterior SC.

6.1. The density function is not monotonically increasing or decreasing

The fact that the density function is not strictly monotonic means that there is more than one minimum in the function in the interval [1,max(v_t)]. This leads to many possible solutions, and the system can get trapped in one that does not maintain topography. For instance, consider the ephrin-A2 gradient reported by Hansen et al. (2004) (see Fig. 5). Here, there are two possible solutions to some of the axons. How could such a gradient still produce single solutions? One possible answer lies in the combination of multiple ligands (see Section 7). In essence, if multiple gradients are combined, the combination of these gradients as perceived by the growth cone may become monotonic even if some of the individual gradients are non-monotonic.

6.2. The density function is linear in the interval [1,*max*(v)]

If the ligand gradient is linear, then the local optimum rule will never go to zero because $\partial L(v_t)/\partial v_t = 1$ for every value of v_t. If the local optimum rule never goes to zero, then the axon will never stop traveling, and eventually "fall off" the target surface. This problem was pointed out by Goodhill (1998a), who concluded that the local optimum rule does not hold for linear ligand gradients. However, this objection to local optimum rules was never framed in the context of the servomechanism model. Recall that, in this model, migration does not occur unless $d_{end} < d_{start}$. Thus, even if the ligand gradient is linear, the axon will never fall off the target surface. Our proposal is that a stop signal can be generated in one of two possible ways. First, as we have argued, the local optimum rule may tell the growth cone that the ligand density is no longer changing, and so it should stop migrating. Second, if, after several trials, d_{end} never gets lower than d_{start} a stop signal may also be generated. In other words, if the axon has sufficiently explored the local environment and can no longer lower d, it may decide to stop at its current position. This proposition may be corroborated by empirical evidence showing that axons tend to stop at a defined ephrin concentration regardless of the slope of the ligand gradient (Rosentreter et al., 1998). Thus, d may itself constitute a second stop signal used by the axon. This signal could resolve the problem of a linear ligand density function by providing a stop signal when the local optimal rule would fail to generate one.

6.3. The density function is flat in some interval [v_1, v_2]

If the density function contains a region that is perfectly flat, i.e., $\partial L(v_t)/\partial v_t = 0$, then the axon could land anywhere within this region with the exact same result in terms of distance. This is a problem similar to having more than one minimum in the ligand density function (see Section 6.1), because it means that there are many possible solutions that are all equivalent. From the point of view of biological systems, it would be desirable to have a combination of mechanisms that insures that, even in the presence of a flat gradient, a population of axons can distribute themselves in a topographically faithful manner across the target surface. An addition to the servomechanism-local optimum rule model that makes this possible is *axonal competition*. According to this mechanism, a growth cone will try and avoid sites of high axonal density by being pushed to neighboring sites (Honda, 2003). While a good deal of biological evidence for the involvement of axonal competition in the development of retinal projections exists (Fraser and Perkel, 1990), the molecular bases of axonal competition are not well understood. In previous work (Thivierge and Balaban, 2005), we have shown that adding axonal competition to the servomechanism-local optimum rule model leads to maps that are topographically faithful despite a flat gradient located over some portion of the ligand surface. This works because, through competition, axons will avoid densely populations regions of the target surface. It is also possible that other mechanisms play a role in distributing axons in a topographical manner along a flat axon. Some of these mechanisms may act through activity-dependent processes, in particular through the refinement that occurs by spontaneous waves of correlated activity on the RGCs (McLaughlin et al., 2003).

Please cite this article in press as: Thivierge, J.-P., Balaban, E., Getting into shape: Optimal ligand gradients for axonal guidance, BioSystems (2006), doi:10.1016/j.biosystems.2006.07.001

6.4. The ligand function is not differentiable at every point

One could argue that the servomechanism-local optimum rules model would never work with real axons, simply because biological systems can have noisy ligand density functions that are not differentiable at every point. For instance, the function shown in Fig. 5 is very wobbly, and thus may contain points where the gradient shifts direction very sharply, thus leading to locations that are not differentiable.

We argue that this should not matter, because sampling of the target surface is *discrete* as opposed to continuous. This means that a traveling axon will experience the ligand density at specific points, not at every possible location. By this discrete sampling, the growth cone constructs an approximation of the ligand density function, one that is smoother than the actual gradient. These ideas will be elaborated in future work.

Growth cone sampling may "smooth out" discontinuities in the shape of the ligand density function, but what about the global shape of the gradient? If the global shape is discontinuous, it may not be possible to differentiate the ligand density function. However, empirical evidence suggests that the global shape of ligand gradients is graded, as opposed to discontinuous (see Hansen et al., 2004 for empirical evidence and a discussion on the topic).

7. Combining multiple ligand gradients

As it stands, our proposed model holds that a single ligand gradient is sufficient to produce topographic maps. In theory, a single gradient may be enough because one given gradient can act both repulsively and attractively, depending on the concentration of receptor signal at the growth cone (Hansen et al., 2004). However, a model that employs a single gradient is overly simplistic. Several molecular gradients have been found on the SC, including members of the Eph family and others of a different nature. How can a number of gradients interact and contribute to axonal guidance? In addition, why do a multitude of gradients exist, when our theoretical analysis (as well as some experimental data) shows that a single gradient could suffice? The answer to these questions may be found by exploring a limitation of the model having to do with the non-monotonicity of ligand density functions (see Section 6.1). Although some non-monotonic gradients have been found empirically (e.g., Fig. 5), our model is unable to achieve a topographic map with them. Hence, the model may be overly simplistic in its assumption of a single ligand gradient, which cannot produce topographically correct maps if the gradient is non-monotonic.

Would adding more ligand gradients take care of both these problems at once? In our model, two gradients can be combined through their multiplicative interaction. In this way, the effective gradient $E(v_t)$ given multiple ligand gradients $L_i(v_t)$ is computed according to

$$E(v_t) = \prod_i L_i(v_t). \tag{13}$$

Fig. 6a shows the effective gradient resulting from the combination of two ligand gradients, namely the gradient given by Eq. (10), and a non-monotonic parabolic gradient (Fig. 6a). As depicted, the effective gradient is an "average" of the two ligand gradients from which it is formed. This effective gradient takes on characteristics of the two ligand gradients; it is overall descending, but slightly non-monotonic towards the posterior end. Thus, combining a monotonic and a non-monotonic ligand gradient may result in an effective gradient that is only slightly non-monotonic. Following this initial intuition that adding more gradients may render the effective gradient more monotonic, combining a non-monotonic ligand gradient with several monotonic ligand gradients can further accentuate the effect shown in Fig. 6a (shown in Fig. 6b). Here, the monotonic gradients are added by subtracting a small factor ϕ between $[1, 4]$ from Eq. (10), thus changing the equation to

$$L(v_t) = \left(\frac{\sqrt{0.5|uv_t - M_u|}}{u} \right) - \phi.$$

As a result, the effective gradient becomes monotonic, by flattening out towards the posterior end. These results demonstrate that it is possible to obtain a monotonic effective gradient even if not all of the ligand gradients present on the target surface are strictly monotonic.

Thus, we can speculate that a monotonic effective gradient obtained through the combination of several ligand gradients depends on one of two possibilities: (1) either the majority of gradients are monotonic, or (2) the monotonic gradients have more impact than their non-monotonic counterparts. Either of these two possibilities will result in an effective gradient that is close to monotonic. The effective gradient of Eq. (10) tells us nothing about the shape of the individual ligand gradients that are composing it. Rather, this equation gives us the shape of the gradient experienced by the growth cone as a result of combining all the ligand gradients present on the target surface. Theoretical speculations regarding constraints on individual ligand gradients were described in the above paragraph (i.e., most should be monotonic).

Please cite this article in press as: Thivierge, J.-P., Balaban, E., Getting into shape: Optimal ligand gradients for axonal guidance, BioSystems (2006), doi:10.1016/j.biosystems.2006.07.001

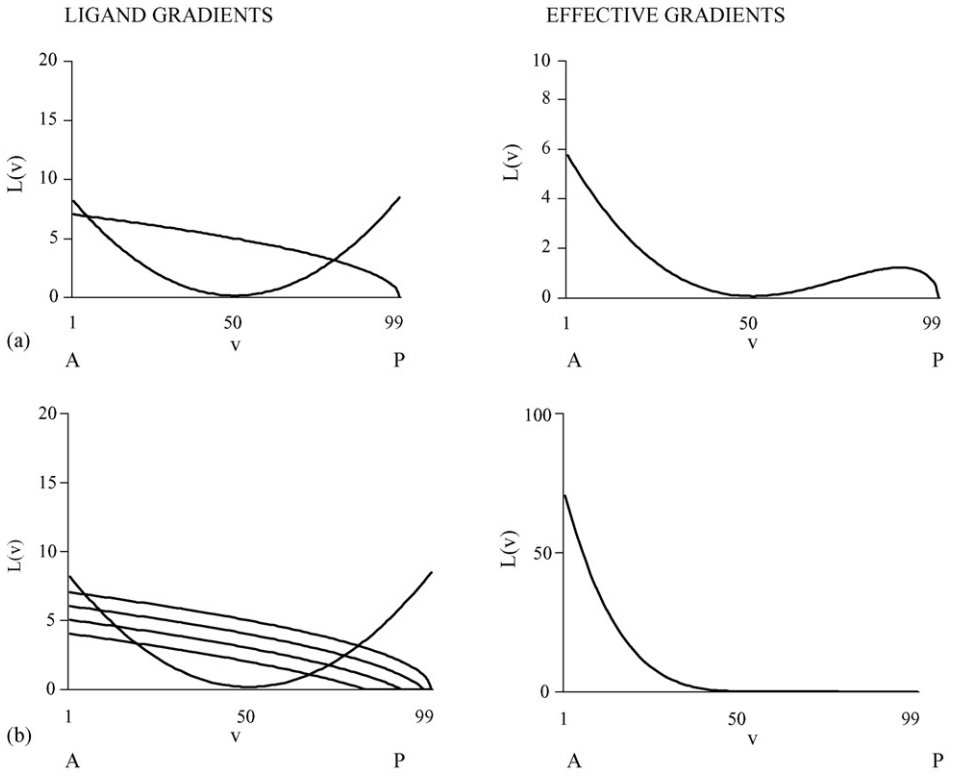

Fig. 6. Combinations of ligand density functions and resulting effective gradients. In (a), a parabolic gradient is combined with the monotonic gradient of Eq. (10). The gradients are combined using Eq. (13). In (b), the same parabolic gradient is combined with four monotonic gradients obtained from Eq. (10). As a result of adding more monotonic gradients, the effective gradient becomes more monotonic. P = posterior SC; A = anterior SC.

8. Repellent and counter-repellent forces

One possible interpretation of the gradient proposed in Eq. (10) is that it constitutes an abstract signal that can be further decomposed into repulsive and counter-repulsive forces acting on the growth cone. Conceptualizing a signal according to these forces allows a computational model to abstract away from molecular gradients, towards more fundamental kinetic forces of attraction and repulsion. This conceptualization possesses several advantages. Importantly, it avoids the problem of missing information about the shape of some molecular gradients acting on migration. Although some authors have suggested mathematical functions to fit some of the known molecular gradients in mice (Reber et al., 2005), these functions describe only a few of the molecules binding to the growth cone receptors. At the current time, the exact distribution of all these molecules is not known, and neither is their interaction with growth cone receptors. Instead of attempting to approximate the individual gradient of several molecules, the proposed model combines various subtypes of Ephs and ephrins into two functions representing repellent and counter-repellent forces applied to the growth cone. This approach is similar in spirit to that of Yates et al. (2004), whose model combines the various subtypes of EphAs and ephrin-As into single curves, on the basis that ephrin-A2 and -A5 molecules can bind and activate all of the EphAs expressed by RGCs (i.e., EphA4–A6 in mice; Brown et al., 2000). Through the use of a single repellent and a single counter-repellent gradient, the proposed model abstracts away from: (1) the number of gradients that may bind to growth cone receptors; (2) the kind of molecules involved; (3) the way in which these molecules interact; (4) whether individually they are repellent or counter-repellent; (5) their specific individual concentrations.

In order to capture both attractant and repulsive forces, several observations are necessary. First, at low concentrations of ligand, an attraction force is present, and the strength of the repellent force is null. Second, at higher concentrations of ligand (past a given threshold θ), the repellent force begins an exponential increase. According to a recent view (Hansen et al., 2004), a TZ is established at the location where repellent and counter-repellent forces counter-balance.

Please cite this article in press as: Thivierge, J.-P., Balaban, E., Getting into shape: Optimal ligand gradients for axonal guidance, BioSystems (2006), doi:10.1016/j.biosystems.2006.07.001

In Section 4, we have discussed how axons from different locations of the retina may experience SC gradients in very different ways, thus arguing that effective gradients can emerge out of the interaction of receptor and ligand gradients. This view may impact on they way in which attractant and repulsive forces influence migration. At certain concentrations of ligands, and given particular receptor densities, growth may be either promoted or inhibited. Eq. (10) fits well with this idea, because the shape of the ligand gradient is dependent upon the position u of the axon on the retina.

An equilibrium point p between attractant and repellent forces is defines as a location on the SC where $E(v_t) = I(v_t)$. In the current description, we make the equilibrium point correspond to the middle point between u and the threshold θ below which no repulsion is possible (in practice, however, the middle point can fall anywhere between θ and u). Knowing u and θ, we find:

$$p = u - 0.5(u - \theta). \tag{14}$$

In sum, three sets of observations can be generated that will help find the equilibrium point:

(1) between $v_t = 0$ and $v_t = u$, the attractant signal is inversely proportional to the ligand gradient.
(2) between $v_t = 0$ and $v_t = \theta$, the repellent signal is constant at zero.
(3) between the threshold $v_t = \theta$ and the equilibrium point $v_t = p$, the repellent signal becomes inversely proportional to the ligand gradient.

The equilibrium point is defined as the location on the tectum where the attractant and repellent forces balance out (if these forces are represented as functions, this is the point on a graph where the two lines would cross). Hence, the relationship between the two curves directly determines the location of the equilibrium point. It is assumed here that both forces exert equal but opposite pulls on the growth cone. Thus, equilibrium points represent locations on the target surface where both functions exert the same force on the growth cone.

In order to show the interaction of these forces, an equation for each must be defined. For this purpose, a counter-repellent signal a repellent signal $E(v_t)$ is obtained through a linear signal:

$$E(v_t) = \alpha v_t, \tag{15}$$

with the value of $\alpha = 0.08$. The repellent signal $I(v_t)$ is based on the non-linear ligand gradient of Eq. (10), and insures that $I(\theta) = 0$. Hence, to obtain this function, we perform the following transformation over Eq. (10):

$$I(v_t) = \left| \left(\frac{\sqrt{0.5|u v_t - M_u|}}{u} \right) - \left(\frac{\sqrt{0.5|u\theta - M_u|}}{u} \right) \right|. \tag{16}$$

For simplification purposes, only the repellent function $I(v_t)$ is made dependent upon receptor density, and not the attraction function $E(v_t)$. However, it is conceivable that both equations could be made dependent upon receptor density.

Fig. 7 shows examples of attractant and repellent signals using different values of u. In this figure, we set $\theta = u^{0.5}$, $M_u = u^2$, and p according to Eq. (14). The equilibrium points correspond to TZs that maintain topography (with correct polarity). This topography emerges naturally by using the effective gradient of Eq. (10) as a repellent force (cf., Eq. (16)).

Of course, there are other ways to obtain an equilibrium point mathematically. One advantage of the proposed method is that, under their current forms, the attractive and repellent functions bear a close resemblance to those of Hansen et al. (2004), who based their model on direct empirical evidence. However, the exact slopes of the attractant and repellent signals remain to be determined empirically.

One feature of the proposed model emerges when comparing the equilibrium point of $I(v_t)$ and $E(v_t)$ with the effective gradient $L(v_t)$. As depicted in Fig. 7, minima of $L(v_t)$ are always found at locations more posterior. As a result, axons will initially overshoot the equilibrium in their migration behavior. This finding has been observed with in vivo mouse axons (Yates et al., 2001). The proposed model offers a natural account of overshooting during retinotopic development. This account does not artificially impose overshooting on the migrating axons. Rather, overshooting emerges from the interaction of a stopping rule with attractant–repellent forces.

The initial overshooting of axons leads to the establishment of a TZ at an unstable point where repellent forces dominate over attractant forces. As discussed next, it is necessary to introduce a mechanism to allow growth cones to retract to the equilibrium point. We will show how retraction is possible through backbranching.

9. Interstitial branching

In the described servomechanism model, axons migrate towards a point where a local optimum rule is met. Because, past this point, it not possible for growth cones to detect further increases in ligand density, a stop signal is triggered. However, at the location where

Please cite this article in press as: Thivierge, J.-P., Balaban, E., Getting into shape: Optimal ligand gradients for axonal guidance, BioSystems (2006), doi:10.1016/j.biosystems.2006.07.001

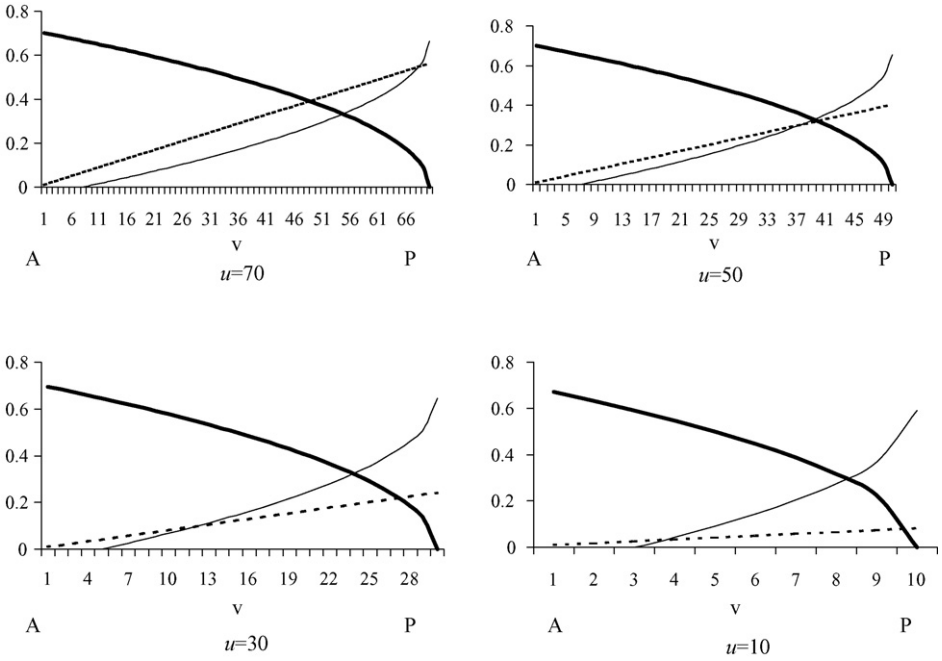

Fig. 7. Attraction and repellence contributions of ligand gradient across a target surface. Thin solid line: repellent forces $I(v_t)$; thin dashed line: attractant force $E(v_t)$; thick solid line: effective gradient $L(v_t)$. Absolute values of $I(v_t)$ are plotted for ease of interpretability (these values are otherwise negative). P = posterior SC; A = anterior SC.

migration stops, growth cones have overshot the point of equilibrium where repellent and counter-repellent forces are counter-balanced. This behavior of the model motivates the use of a mechanism that retracts axons to correct TZs located at equilibrium. This retraction will be made possible through backbranching.

In backbranching, novel interstitial branches are established along the main axonal shaft. In the proposed model, the probability that a branch will be formed or not at a given location is dependent upon the repellent and counter-repellent forces of Eqs. (15) and (16). In this way, the formation of interstitial branches will be maximally promoted at locations of equilibrium, and gradually less promoted at locations that are away from equilibrium. After some time, this process will result in a proportionally denser arborisation at the location of equilibrium than at the location where migration was initially stopped. At a later stage of development (not modeled here), this difference may incite activity-dependent mechanisms towards retraction of the growth cone, stabilization of the TZ at the point of equilibrium, and pruning of extranumerary connections (Ruthazer and Cline, 2004).

A computational approach to performing backbranching has been proposed by Yates et al. (2004) and was designed to capture several findings from Yates et al. (2001). This approach takes into account that a high number of arbors can form from branches that develop off the main axon, and that these arbors can themselves further divide, and so on. By this division, a high number of sub-branches increases the likelihood of adding further branches. This is captured through a function $D(v_t)$, reflecting the branch density of an axon at position v_t on the target surface:

$$D(v_t) = \left(1 - \frac{\alpha}{1 + e^{-(t-\gamma)/\beta}}\right) + \left[\frac{\alpha}{1 + e^{-(t-\gamma)/\beta}} \frac{\sum_{w_t=v_t-10}^{v_t+10} \sigma S(w_t)}{\sum_{w_t=1}^{100} S(w_t)}\right], \quad (17)$$

with constant parameters $\sigma = 0.5, \alpha = 0.7, \rho = 2.0, \theta = 0.7$, $\gamma = 7, \beta = 10$, and $\eta = 0.35$ (taken from Yates et al., 2004). The probability that an axon will branch at a location v_t is obtained through the following calculation:

$$p(v_t) = \eta(1 - (I(v_t) - E(v_t))^{\varphi})D(v_t), \quad (18)$$

with constant parameter $\varphi = 0.1$. This probability reflects the influence of both the $I(v_t)$ repellent and $E(v_t)$ counter-repellent functions in branching behavior. More specifically, Eq. (18) promotes branch formation at the point of equilibrium between $I(v_t)$ and $E(v_t)$. This feature constitutes a novel approach to branch formation; in

Please cite this article in press as: Thivierge, J.-P., Balaban, E., Getting into shape: Optimal ligand gradients for axonal guidance, BioSystems (2006), doi:10.1016/j.biosystems.2006.07.001

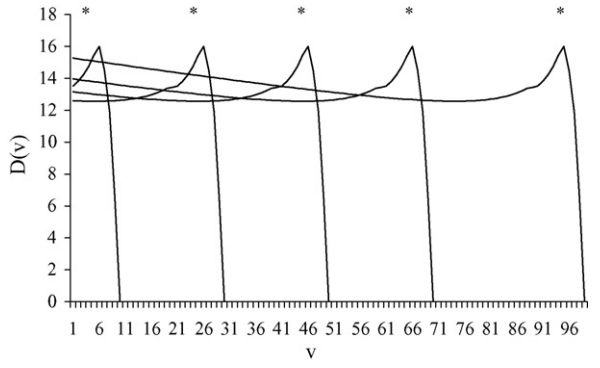

Fig. 8. Branch density of six projecting axons ($N=6$). After initial overshooting, interstitial branches start forming at a location of equilibrium (indicated by an asterisk "*") anterior to the initial TZs. From left to right: $u=\{10, 30, 50, 70, 100\}$. Initially, all axons enter the target surface from the same $v_{t=1} = 1$ location. Then, for each time-step until $t=100$, migration through the servomechanism model occurs concurrently with growth in branch density using Eqs. (17)–(19).

the original model (Yates et al., 2004), branch formation was under the influence of a repellent function alone.

A total arbor size $S(w_t)$ can be obtained as the sum of all branch segments extending from an axon at SC locations w_t, where w_t can take on different values of v_t according to Eq. (17). The value of $S(w_t)$ is initialized at zero in all simulations, and updated as follows:

$$S(w_t) = N[S(w_t) + p(w_t)], \tag{19}$$

where N is the total number of projections migrating from the start location, and is used as a scaling factor.

The goal of backbranching is to extend interstitial branches along the main axonal shaft. Through this process, a high density of branches is formed at the equilibrium point where the repellent and counter-repellent forces balance out, and a low density of branches is formed at the location where the local optimum rule is met (Fig. 8). Through a combination of servomechanism guidance and backbranching, activity-independent processes provides a rough bias towards topography. As a result, projecting axons exhibit the highest density of projections at equilibrium sites. Because axons from different projecting sites on the retina are guided towards different equilibrium sites on the SC, this results in a topographic organization of projections. However, because of the density of branches that is also formed at locations other than the equilibrium sites, the projections do not display a strictly point-to-point mapping. It is postulated that other mechanisms, including activity-dependent processes (McLaughlin et al., 2003; McLaughlin and O'Leary, 2005) are responsible for refining topography by pruning out extranumerary connections and thus refining the TZ arbors.

There are a few assumptions to the proposed backbranching mechanism that constitute simplifications of the underlying physiological processes involved, and thus are not fully representative of the phenomenon modeled. One of these assumptions is that the same molecular mechanisms that are responsible for axonal guidance are also responsible for backbranching. In this way, the molecular gradients responsible for migration of the growth cone are also responsible for generating repellent and counter-repellent signals that promote or inhibit interstitial branch formation. This assumption is taken as a mechanistic simplification of a process that actually involves several interacting processes. Another limit of the proposed account is that no explanation is provided for branch stabilization. In other words, the mechanisms that allow branches to stop growing and subdividing further are not described. Branch stabilization may be attributed to different molecular cues that are independent of the ones described here (for instance, BDNF, see Hu et al., 2005). Finally, one last assumption of the backbranching mechanism proposed is that branch formation along a given axon does not influence branch formation along other axons. Conceivably, this assumption may be broken in natural systems, by mechanisms that perform cell–cell attraction and repulsion among branches.

10. Conclusions

In this paper, we have described how a combination of servomechanism guidance and local optimum rules can lead to optimal topographic maps. The model was developed based on new experimental evidence suggesting that different cells make different interpretations of the same ligand density functions according to the receptor densities on their growth cones (Hansen et al., 2004). Some new hypotheses were discussed, and can be summarized as follows. First, the effective gradient is dependent upon the receptor density of the growth cone, as well as its maximum receptor saturation. As a result, different growth cones will experience different effective gradients, even if, in fact, the actual ligand density function is unchanged. Second, if many ligands are present on the target surface, the model predicts that either there are many more monotonic gradients than non-monotonic, or that the monotonic gradients have more impact on migration than their non-monotonic counterparts.

One advancement of the model is that it proposes conditions under which set-point and local optimum rules are equivalent. This is achieved by making the ligand gradient directly dependent upon the receptor density of the growth cone. In addition, some conditions are

Please cite this article in press as: Thivierge, J.-P., Balaban, E., Getting into shape: Optimal ligand gradients for axonal guidance, BioSystems (2006), doi:10.1016/j.biosystems.2006.07.001

proposed under which some previously proposed relationships between receptor and ligand densities might be altered and still yield topographic organization. In particular, under certain values of maximum receptor saturation, it is possible to generate proportional receptor and ligand gradients; under other values of maximum receptor saturation, it is possible to generate receptor and ligand gradients with inverse proportionality.

One issue of debate with respect to molecular guidance has to do with the relative versus absolute nature of the signaling cues provided. On the one hand, some accounts suggest that relative signaling is required to account for knock-out data (Brown et al., 2000; Reber et al., 2005). On the other hand, alternative accounts have suggested that absolute signaling may also account for the same data (Koulakov and Tsigankov, 2004). Our current position lies somewhere in between, as both perspectives are compatible with our proposed model. In the proposed model, growth cones are sensitive to both differences in molecular concentrations across the target surface as well as absolute concentrations. Prior to reaching maximum receptor saturation, growth cones are guided by relative signaling. Accordingly, growth cones will tend towards locations where the maximum receptor saturation is relatively higher compared to previously sampled locations. The maximum receptor saturation point constitutes an absolute location beyond which the growth cone is unable to detect further increases in molecular concentrations. In the proposed account, the nature of the stop signal is also compatible with both absolute and relative signaling. According to the local optimum rule, a stop signal is triggered when the growth cone no longer detects differences in molecular concentration in its progression across the target surface. Thus, it is a relative difference in signal that generates the stop signal. However, it could also be argued that it is an absolute difference in signal that is responsible for the stop signal, since after the growth cone reaches maximum receptor saturation, it no longer detects differences in molecular concentration. In sum, the model suggests that both absolute and relative accounts of molecular signaling can describe the same underlying process.

Despite some advances, our proposed model is far from definitive; rather, it is an initial proposal that we intend to extend and refine further. One limitation of the proposed account is that it is agnostic as to how a growth cone detects gradients. This question has been addressed in other models (e.g., Goodhill et al., 2004). Finally, some more direct comparisons will be required in order to better evaluate differences between the current account and previously proposed models.

Acknowledgments

This research is supported by a doctoral fellowship from FQRNT to the first author. This work benefited from discussions with Edward S. Ruthazer (Montreal Neurological Institute), as well as the comments of anonymous reviewers.

References

Brown, J.E., et al., 2000. Tospographic mapping from the retina to the midbrain is controlled by relative but not absolute levels of EphA receptor signaling. Cell 102, 77–88.

Cheng, H.J., Nakamoto, M., Bergemann, A.D., Flanagan, J.G., 1995. Complementary gradients in expression and binding of ELF-1 and Mek4 in development of the topographhic retinotectal projection map. Cell 82, 371–381.

Feldheim, D.A., et al., 1998. Topographic guidance labels in a sensory projection to the forebrain. Neuron 21, 1303–1313.

Fraser, S.E., Perkel, D.H., 1990. Competitive and positional cues in the patterning of nerve connections. J. Neurobiol. 21, 51–72.

Goodhill, G.J., 1998a. Gradients for retinotectal mapping. Adv. Neural Inf. Process. Syst. 10, 152–158.

Goodhill, G.J., 1998b. Mathematical guidance for axons. Trends Neurosci. 21, 226–231.

Goodhill, G.J., Gu, M., Urbach, J.S., 2004. Predicting axonal response to molecular gradients with a computational model of filopodial dynamics. Neural Comput. 16, 2221–2243.

Goodhill, G.J., Richards, L.J., 1999. Retinotectal maps: molecules, models and misplaced data. Trends Neurosci. 22, 529–534.

Goodhill, G.J., Urbach, J.S., 1999. Theoretical analysis of gradient detection by growth cones. J. Neurobiol. 41, 230–241.

Goodhill, G.J., Xu, J., 2005. The development of retinotectal maps: a review of models based on molecular gradients. Netw.: Comput. Neural Syst. 16, 5–34.

Gordon-Weeks, P.R., 2000. Growth Cones: The Molecular Approach to Their Behavior. Cambridge University Press.

Hansen, M.J., et al., 2004. Retinal axon response to ephrin-As shows a graded, concentration-dependent transition from growth promotion to inhibition. Neuron 42, 717–730.

Honda, H., 1998. Topographic mapping in the retinotectal projection by means of complementary ligand and receptor gradients: a computer simulation study. J. Theor. Biol. 192, 235–246.

Honda, H., 2003. Competition between retinal ganglion axons for targets under the servomechanism model explains abnormal retinocollicular projection of eph receptor-overexpressing or ephrinlacking mice. J. Neurosci. 23, 10368–10377.

Hu, B., Nikolakopoulou, M., Cohen-Cory, S., 2005. BDNF stabilizes synapses and maintains the structural complexity of optic axons in vivo. Development 132, 4285–4298.

Koulakov, A.A., Tsigankov, D.N., 2004. A stochastic model for retinocollicular map development. BMC Neurosci. 5, 3–30.

Loschinger, J., Weth, F., Bonhoeffer, F., 2000. Reading of concentration gradients by axonal growth cones. Philos. Trans. Roy. Soc. Lond.: Biol. Sci. 355, 971–982.

McLaughlin, L., 1981. Two at Harvard share Nobel prize in medicine. Boston Globe 10, 1.

McLaughlin, T., O'Leary, D.M., 2005. Molecular gradients and development of retinotopic maps. Annu. Rev. Neurosci. 28, 327–355.

Please cite this article in press as: Thivierge, J.-P., Balaban, E., Getting into shape: Optimal ligand gradients for axonal guidance, BioSystems (2006), doi:10.1016/j.biosystems.2006.07.001

McLaughlin, T., Torborg, C.L., Feller, M.B., O'Leary, D.M., 2003. Retinotopic map refinement requires spontaneous retinal waves during a brief critical period of development. Neuron 40, 1147–1160.

Palmer, A., Klein, R., 2003. Multiple roles of ephrins in morphogenesis, neuronal networking, and brain function. Genes Dev. 17, 1429–1450.

Reber, M., Burrola, P., Lemke, G., 2005. A relative signalling model for the formation of a topographic neural map. Nature 431, 847–853.

Rosentreter, S.M., et al., 1998. Response of retinal ganglion cell axons to striped linear gradients of repellent guidance molecules. J. Neurobiol. 37, 541–562.

Ruthazer, E.S., Cline, H.Y., 2004. Insights into activity-dependent map formation from the retinotectal system: a middle-of-the-brain perspective. J. Neurobiol. 59, 134–146.

Sperry, R., 1963. Chemoaffinity in the orderly growth of nerve fiber patterns and connections. Proc. Natl. Acad. Sci. U.S.A. 50, 703–710.

Thivierge, J.P., Balaban, E., 2005. Faithful retinotopic maps with local optimum rules, axonal competition, and hebbian learning. In: Proceedings of the IEEE International Joint Conference on Neural Networks, pp. 2760–2765.

Yates, P.A., Roskies, A.L., McLaughlin, T., O'Leary, D.D.M., 2001. Topographic-specific axon branching controlled by ephrin-As is the critical event in retinotectal map development. J. Neurosci. 21, 8548–8563.

Yates, P.A., et al., 2004. Computational modeling of retonotopic map development to define contributions of Eph-A–ephrinA gradients, axon–axon interactions, and patterned activity. J. Neurobiol. 59, 95–113.

Please cite this article in press as: Thivierge, J.-P., Balaban, E., Getting into shape: Optimal ligand gradients for axonal guidance, BioSystems (2006), doi:10.1016/j.biosystems.2006.07.001